Novel Dual-Airgap Axial Field Fault-Tolerant Flux Switching Permanent Magnet Machines with High Torque Performance.

W. ZHAO[1], T. A. LIPO[2], B. KWON[1]
1. Electronic Systems Engineering, Hanyang University, Ansan, Korea; 2. Electrical and Computer Engineering, University of Wisconsin-Madison, Madison, WI

I. INTRODUCTION

In recent years, flux switching permanent magnet machines (FSPMMs) have been comprehensively investigated for various applications [1]-[2]. In particular, the axial field FSPMMs are attracting much attentions due to the incorporation of the advantages of FSPMMs and axial filed permanent magnet (PM) machines, which offer the merits of high torque/power density, high efficiency, compact construction and good heat dissipation [3]. However, the axial field FSPMMs generally exhibit high cogging torque and torque ripple resulting from the double salient structure and high airgap flux density by the flux focusing effects, while it is necessary to reduce the pulsating torques for high-performance applications such as servo motors and direct-drive wind power generators [4]. Furthermore, the FSPMMs show good potentials to be in-wheel direct drive motors, wherein the fault-tolerant capability is always essential to be further improved to spread them for transportation applications [5].

Therefore, in this paper, a novel axial field FSPMM is proposed for obtaining good fault-tolerant capability and high torque performance with not only high torque density but also low cogging torque and torque ripple. The proposed FSPMM is equipped with two unaligned rotors with one tooth width offset, and two sets of phase-group concentrated-coil windings, for obtaining improved fault-tolerant capability and dramatic flux magnification. In order to highlight the contribution of the proposed FSPMM, two conventional FSPMMs are adopted as the reference models and the performance comparison is performed based on 3-D finite element method (FEM).

II. MODELING AND FEM ANALYSIS RESULTS

In Fig. 1, the conventional single-airgap axial field FSPMM having 12 stator slots/10 rotor poles (model 1) and dual-airgap axial field FSPMM having 12 stator slots/14 rotor poles (model 2) with concentrated windings are given as the reference models. The proposed dual-airgap axial field FSPMM having 12 stator slots/13 rotor poles (model 3) with phase-group concentrated-coil windings is shown Fig. 2. All the machines are kept as the same size and similar weight as listed in Table I. The ferrite permanent magnets are embedded in the stator with circumferentially magnetized direction. The superiority of the proposed model is illustrated in Fig. 3 and 4. As shown in the design sketch of Fig. 3, a series of teeth are constructed to be in group with the same phase winding, while the slot and teeth width within one phase group are designed to be the same as $\pi/2$ (elec.), whereas the slot width between two different phases is $5\pi/6$ (elec.) for producing a three-phase balanced back EMF. Together with the unaligned arrangement of the two rotors, within one phase group, almost the total PM flux will follow into one airgap when the rotor pole rotates to become aligned with the upper/lower teeth of stator. Thus, a highly improved airgap flux density resulting in a high resultant torque can be obtained as illustrated in Fig. 4. Due to the alternate operating principle for PM flux concentration, the phase back EMFs produced in the upper and lower stator windings will be shifted by $\pi/2$ (elec.), contributing to a dual three-phase channel for improved fault-tolerant capability.

Fig. 5 and Fig. 6 show the torque characteristic of the proposed FSPMM by 3-D FEM. In a large operating range of current density (J), the torque ripple of the proposed model is suppressed to be below 8.5%. Fig 7 and 8 show the comparison of cogging torque and electromagnetic torque among the conventional and proposed FSPMMs. As listed in Table I, the proposed model 3 has significant improvements of average torque, torque density and power density (power-weight ratio) at the current density of 8 Arms/mm^2, while has the dramatic reduction of cogging torque and torque ripple when compared to the conventional model 1 and model 2.

III. CONCLUSION

This paper has proposed a novel dual-airgap axial filed FSPMM providing with good fault-tolerant capability and high torque performance by utilizing two sets of phase-group concentrated-coil windings and the unaligned arrangement of two rotors. Based on 3-D FEM analysis results, it shows the proposed model exhibits high torque performance in a large operating range of current density. Compared to the two reference models, the proposed model shows significantly improved torque/power density as well as reduced cogging torque and torque ripple.

[1] Z. Q. Zhu and J. T. Chen, "Advanced flux-switching permanent magnet brushless machines," *IEEE Trans. Magn.*, vol. 46, no. 6, pp. 1447–1453, Jun. 2010.
[2] R. Cao, C. Mi, and M. Cheng, "Quantitative comparison of flux-switching permanent magnet motors with interior permanent magnet motor for EV, HEV, and PHEV applications," *IEEE Trans. Magn.*, vol. 48, no. 8, pp. 2374–2384, Aug. 2012.
[3] L. Hao, M. Lin, X. Zhao, X. Fu, Z. Q. Zhu, and P. Jin, "Static characteristics analysis and experimental study of a novel axial field flux switching permanent magnet generator," *IEEE Trans. Magn.,* vol. 48, no. 11, pp. 4212–4215, Nov. 2012.
[4] W. Fei, P. C. K. Luk, and J. X. Shen, "Torque analysis of permanent magnet flux switching machines with rotor step skewing," *IEEE Trans. Magn.,* vol. 48, no. 10, pp. 2664–2673, Oct. 2012.
[5] X. Xue, W. Zhao, J. Zhu, G. Liu, X. Zhu, and M. Cheng, "Design of five-phase modular flux-switching permanent-magnet machines for high reliability applications," *IEEE Trans. Magn.,* vol. 49, no. 7, pp. 3941-3945, 2013.

Fig. 1 Topologies of the conventional FSPMMs

Fig. 2 Topology of the proposed FSPMM

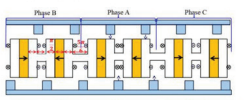

Fig. 3 Design sketch of the proposed FSPMM

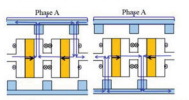

Fig. 4 Operating principle of the proposed FSPMM

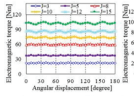

Fig. 5 Torque profile

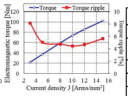

Fig. 6 Torque and torque ripple

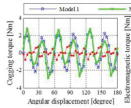

Fig. 7 Cogging torque

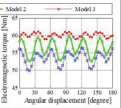

Fig. 8 Electromagnetic torque

Table I Specifications and FEM analysis results

Items	Unit	Model 1	Model 2	Model 3
Slots/Poles	-	12/10	12/14	12/13
Machine outer diameter	mm	255		
Axial length	mm	106		
Airgap length	mm	1.2		
Phase coil turns	-	192		
Machine weight	kg	21.8	22.8	22.2
Rated speed	rpm	450		
Current density	A/mm^2	8		
Cogging torque	Nm	4.823	5.712	1.634
Torque (average)	Nm	53.5	56.4	60.1
Torque ripple	%	12.8	13.7	3.7
Torque density	Nm/L	9.9	10.4	11.1
Power @450rpm	kW	2.52	2.66	2.83
Power density	kW/kg	0.115	0.117	0.128
Efficiency	%	82.0	81.8	82.7